Cell Stress and Chaperones (2015) 20:697–708
DOI 10.1007/s12192-015-0597-9

ORIGINAL PAPER

Caco-2 cells infected with rotavirus release extracellular vesicles that express markers of apoptotic bodies and exosomes

Diana Bautista[1] · **Luz-Stella Rodríguez**[2] · **Manuel A. Franco**[2] · **Juana Angel**[2] · **Alfonso Barreto**[1]

Received: 26 December 2014 / Revised: 24 April 2015 / Accepted: 30 April 2015 / Published online: 15 May 2015

Abstract Previously, we showed that infecting human intestinal epithelial cells (Caco-2) with rotavirus (RV) increases the release of extracellular vesicles (EVs) with an immunomodulatory function that, upon concentration at 100,000×*g*, present buoyant densities on a sucrose gradient of between 1.10 to 1.18 g/ml (characteristic of exosomes) and higher than 1.24 g/ml (proposed for apoptotic bodies). The effect of cellular death induced by RV on the composition of these EV is unknown. Here, we evaluated exosome (CD63, Hsc70, and AChE) and apoptotic body (histone H3) markers in EVs isolated by differential centrifugation (4000×*g*, 10,000×*g*, and 100,000×*g*) or filtration/ultracentrifugation (100,000×*g*) protocols. When we infected cells in the presence of caspase inhibitors, Hsc70 and AChE diminished in EVs obtained at 100,000×*g*, but not in EVs obtained at 4000×*g* or 10,000×*g*. In addition, caspase inhibitors decreased CD63 and AChE in vesicles with low and high buoyant densities. Without caspase inhibitors, RV infection increased exosome markers in all of the EVs obtained by differential centrifugation. However, CD63 preferentially localized in the 100,000×*g* fraction and H3 only increased in EVs concentrated at 100,000×*g* and with high buoyant densities on a sucrose gradient. Thus, RV infection increases the release of EVs that, upon concentration at 100,000×*g*, are composed by exosomes and apoptotic bodies, which can partially be separated using sucrose gradients.

✉ Alfonso Barreto
alfonso.barreto@javeriana.edu.co

[1] Grupo de Inmunobiología y Biología Celular, Departamento de Microbiología, Facultad de Ciencias, Pontificia Universidad Javeriana, Bogotá, Colombia

[2] Instituto de Genética Humana, Facultad de Medicina, Pontificia Universidad Javeriana, Bogotá, Colombia

Keywords Extracellular vesicles · Exosomes · Apoptotic bodies · Caco-2 · Rotavirus · Histone 3

Introduction

Although extracellular vesicles (EVs) were initially considered cellular debris with no importance and with by-product artifacts of the manipulation of cells (Bobrie et al. 2011), their study has become a topic of active research in recent years (Thery 2011). Among the EVs, exosomes are endocytic vesicles composed of a lipid bilayer that contains transmembrane proteins and enclose hydrophilic components from the cytosol of the cell from which they are derived (Thery et al. 2009). These features make EVs effective intercellular transport vehicles (Simpson et al. 2009). However, there are other vesicles that originate from the shedding of the plasma membrane, such as microvesicles and apoptotic bodies formed from an apoptosis process (Mathivanan et al. 2010; Meckes and Raab-Traub 2011; Thery et al. 2009). Several in vitro studies have suggested that these EVs participate in many biological processes, such as angiogenesis, metastasis, cell proliferation, gene regulation, coagulation, pathogen propagation, and immune response (Bobrie et al. 2011; Meckes and Raab-Traub 2011). However, there are limited studies of the in vivo functions associated with EV, which is partially due to the lack of knowledge of their biogenesis process (Ostrowski et al. 2010). In addition, in vitro studies are technically limited because of the low possibility of obtaining pure EV preparations (Bobrie et al. 2012a, 2011; 2012b). Therefore, strategies must be developed to improve the characterization and optimize the isolation procedures of EV subpopulations (Bobrie et al. 2012a, 2011, 2012b).

The identification of proteins related to different biological processes associated with EVs can be useful in the

implementation of strategies to characterize the in vivo function of the EV. Exosomes have been extensively typified through proteomic studies coupled to one-dimensional (1D) and two-dimensional (2D) gels (Kalra et al. 2012) and characteristic markers such as CD63, Hsc70, MFG-E8, and AChE (Bastos-Amador et al. 2012b; Bobrie et al. 2012a; Cantin et al. 2008; Johnstone et al. 1987; Mathivanan et al. 2010) have been identified. Apoptotic bodies have received limited characterization with histones being the best markers recognized so far (Mathivanan et al. 2010; Thery et al. 2001; Xie et al. 2009). Separating the different types of EVs is difficult because they sediment at similar centrifugation velocities, for example, exosomes sediment between 100,000×*g* and 200,000×*g* and float in a sucrose gradient between 1.10 and 1.19 g/ml (Barreto et al. 2010; Gyorgy et al. 2011; Thery et al. 2006); microvesicles sediment between 10,000×*g* and 20,000×*g* and float at 1.16 g/ml (Cocucci et al. 2009; Choi et al. 2007); and apoptotic bodies sediment between 1200×*g* and 100,000×*g* and float at densities >1.24 g/ml (Thery et al. 2001).

Previously, we showed that rotavirus (RV) infection of human intestinal epithelial cells (Caco-2) increased the release of EVs, obtained by filtration/ultracentrifugation, with immunomodulating properties on polyclonally activated T cells (Barreto et al. 2010). At these gravities, exosomes are typically concentrated, and it is likely that apoptotic bodies occur in these preparations because the RV induces an apoptosis process in vitro (Bhowmick et al. 2012; Chaibi et al. 2005; Halasz et al. 2010; Martin-Latil et al. 2007) and in vivo (Boshuizen et al. 2003). Indeed, we showed that EVs from RV-infected and non-infected cells were heterogeneous, with morphologies (visualized by electron microscopy) and flotation densities on sucrose gradients described for exosomes (between 1.10 and 1.18 g/ml) and apoptotic bodies (denser vesicles higher than 1.24 g/ml) (Barreto et al. 2010; Thery et al. 2001). Both types of EVs released by RV-infected cells were more efficient at inhibiting T cell proliferation and viability than were those from non-infected cells, and this effect was partially due to TGF-β induced by viral infection (Barreto et al. 2010; Rodriguez et al. 2012). Also, high-density (>1.24 g/ml) EVs released by infected cells had a more pronounced effect on T cell proliferation than EV with exosome densities (between 1.10 to 1.18 g/ml) liberated by the same cells. Thus, the immunomodulating properties of EVs probably depend on viral infection that induces TGF-β and cell apoptosis.

In this study, we characterized EVs released during RV infection of Caco-2 cells in the presence or absence of caspase inhibitors, evaluating the presence of markers described for exosomes and apoptotic bodies, according to differences in their sedimentation rates and their buoyant densities on a linear sucrose gradient. We found that at 100,000×*g*, there is a co-sedimentation of a complex EV population composed of exosomes and apoptotic bodies. According to the decrease of EV markers in the presence of caspase inhibitors and the appearance of histone H3, we propose that apoptotic bodies produced during RV infection sediment at 100,000×*g* and have densities flotation higher than 1.24 g/ml on sucrose gradients. These high-density EVs, which express the histone H3, can have potentially unique immunomodulatory functions.

Materials and methods

Cells and cell culture

The Caco-2 cells (a gift from C. Sapin, INSERM U 538, Universidad Pierre et Marie Curie, Paris, France) (Rodríguez et al. 2009) were cultured in Dulbecco's modified Eagle's medium (DMEM; Invitrogen-Gibco, Grand Island, NY, USA) supplemented with 20 % fetal bovine serum (FBS; Invitrogen-Gibco, Grand Island, NY, USA), 100 μg/ml penicillin-streptomycin, 2 mM L-glutamine, 100 U/ml Hepes, and 0.1 mM non-essential amino acids (Invitrogen-Gibco, Grand Island, NY, USA) and used between passages 70 and 79. The cells used were free of mycoplasma (Mycoplasma detection kit for conventional PCR, VenorGeM; Sigma-Aldrich, St. Louis, MO, USA), and the experiments were performed in the presence of 0.5 μg/ml ciprofloxacin to maintain the cells in that state. The cells were cultured at a 10,000-cells/cm^2 density in cell culture flasks and cultured for 15 days before inoculation (Barreto et al. 2010). For virus titration assays, MA104 cells were cultivated in 8 % FBS-supplemented DMEM.

RV infection

At day 15 post-culture, FBS was removed from the Caco-2 cells, and the cells were washed with serum-free DMEM three times before inoculation with a multiplicity of infection (moi) of five focus forming units (ffu)/cell of the rhesus monkey rotavirus strain (RRV). RRV was obtained from the lysate of infected MA104 cells and was previously tittered on these cells (Narvaez et al. 2005). As a negative control, a non-infected cell lysate (mock) was used. The viral inoculum was prepared by previously activating RRV with 2 μg/ml trypsin for 30 min. Cells were incubated for 45 min with the viral inoculum, and the monolayers were immediately washed twice with serum-free DMEM and maintained with serum-free DMEM for 24 h to determine EV production. Subsequently, the conditioned medium was collected and used for the isolation of EV, lactate dehydrogenase (LDH) determination, and viral titration.

EV isolation

EVs were obtained by filtration/ultracentrifugation or differential centrifugation protocols. In the first protocol, Caco-2 cells supernatant was collected after 24 h of infection with RRV or mock treatment, centrifuged at 300×*g* to eliminate cellular debris, and filtered using 0.22-μm filters (Millipore, Carrigtwohill, Country Cork, Ireland). The filtered supernatant was centrifuged twice at 100,000×*g* (rotor 70-Ti; Beckman Coulter, Inc., Fullerton, CA, USA) for 90 min, and the obtained pellet was re-suspended in an appropriate volume of phosphate buffered saline (PBS pH 7.4) to achieve a final concentration between 300 and 400 times that of the vesicles from the initial supernatant (filtration/ultracentrifugation protocol) (Barreto et al. 2010; Thery et al. 2002). In the second protocol, 24 h supernatants were processed through successive centrifugations. The Caco-2 cells supernatant was centrifuged at 300×*g* and later at 4000×*g* (to eliminate cellular debris and to obtain large vesicles from dead cells), 10,000×*g* (to obtain microvesicles), and 100,000×*g* (to isolate exosomes) (Bobrie et al. 2012a; Thery et al. 2006). In some experiments, the vesicles isolated at 100,000×*g* by the filtration/ultracentrifugation protocol were separated in a linear sucrose gradient (2–0.5 M sucrose, 20 mM HEPES/NaOH, pH 7.2). The EV preparations were placed in the inferior part of the gradient, and the samples were centrifuged at 100,000×*g* for 15 h (rotor SW41; Beckman Coulter, Inc., Fullerton, CA, USA) (Barreto et al. 2010; Thery et al. 2006). Then, 1 ml fractions were recovered and different fractions were pooled and concentrated by ultracentrifugation at 100,000×*g*.

EV marker analysis

Equal volumes of EV preparations were used for comparative analysis. The AChE activity, which has been used as an exosome marker, was measured using an Amplex® Red Acetylcholine/Acetylcholinesterase Assay Kit (Life Technologies-Molecular Probes, Eugene, OR, USA) following the manufacturer's instructions. The samples were read in a Tecan fluorometer (Tecan GENios; Phoenix Research Products, Hayward, CA, USA). In addition, the presence of Hsc70 and CD63 (typical exosome markers), histone H3, (an apoptotic body marker), and the viral protein VP6 were evaluated using Western blot (WB) immunoassays. For this procedure, a previously established protocol was followed (Barreto et al. 2003, 2010).

Apoptosis inhibition assays

To analyze the effect of caspase inhibitors on the Caco-2 cells apoptosis induced by RV, the Caco-2 cells cultured on microscope slides were treated with the caspase inhibitors z-VAD-fmk, z-DEVD-fmk, and z-LEHD-fmk (R&D® Systems) (Martin-Latil et al. 2007) individually at a 10-μM concentration or in a 5, 10, and 20-μM differential concentration cocktail for 1 h. Subsequently, the cells were infected for 45 min with RRV (moi of five) or treated with the mock control preparation. As a positive control, camptothecin (CPT) was used at concentrations of 5, 10, or 20 μM for 12, 18, or 24 h. The inhibitors were maintained throughout the entire procedure, even during virus inoculation. After 12, 18, and 24 h of infection, the cells were stained with phalloidin Alexa-fluor 594 (to stain actin) and DAPI (to stain the cell nucleus) (Life Technologies-Molecular Probes, Eugene, OR, USA); the infection was verified using monoclonal antibody (Mab) anti-RV VP6 followed by an anti-mouse Alexa-fluor 647 antibody (Life Technologies-Molecular Probes, Eugene, OR, USA). Apoptosis was evaluated by counting apoptotic nuclei using an Olympus FluoView FV1000 confocal microscope (Tokyo, Japan).

To analyze the effect of caspase inhibitors on EV production, cultured cells in culture flasks were treated similarly with the 10 μM caspase inhibitor cocktail and inoculated; 24 h post-infection, the supernatants of these cells were collected to obtain EVs by filtration/ultracentrifugation and differential centrifugation protocols. In certain experiments, the EVs were separated by a linear sucrose gradient as previously described (Barreto et al. 2010). The EV preparations were evaluated for the presence of CD63, Hsc70, AChE, and histone H3.

Western blot

Western blots were performed as previously described (Barreto et al. 2010). Samples were prepared in Laemmli buffer with DTT except for CD63 identification. Proteins were separated using 4–12 and 10 % SDS pre-casting gels (BioRad, Hercules, CA) and transferred to PVDF membranes (BioRad, Hercules, CA). Membranes were blocked during 1 h with a Tris-HCl (pH 7.5) solution containing 5 % skim milk and 0.05 % Tween 20. Then, membranes were incubated with appropriated primary antibodies (mouse MoAb anti-Hc70, clon B-6 from Santa Cruz Biotechnology, Santa Cruz, CA; mouse MoAb anti-CD63, clon H5C6 from BD Pharmingen, San Diego, CA; mouse MoAb anti-histone 3, clon 9C10, Cell Signaling Technology; and mouse MoAb anti-RV VP6, clon 1026, a gift from E. Kohli, Université de Dijon, Dijon, France). After washing, membranes were incubated for 50 min with goat anti-mouse IgG conjugated with peroxidase (Peroxidase ImmunoPure, Pierce Biotechnology, Inc., Rockford, IL). Membranes were developed using the chemiluminescence kit Supersignal West Dura Extended Duration (Peroxidase ImmunoPure; Pierce Biotechnology, Inc., Rockford, IL) and CL-XPosure films (Peroxidase ImmunoPure; Pierce Biotechnology, Inc., Rockford, IL).

Viral titration

MA104 cells cultured on flat 96-well plates were infected with the supernatants (activated with 2 μg/ml trypsin (30 min)) of RRV-infected Caco-2 cells that were previously treated or untreated with the inhibitors at different dilutions. After 16 h of infection, the cells were fixed with absolute methanol and treated with mouse anti-VP6 Mab for 45 min at 37 °C; subsequently, a goat anti-mouse biotin antibody was added for 45 min at 37 °C, and streptavidin-peroxidase was added under the same conditions. To reveal the focus forming units (ffu), an AEC kit (3-amino-9-ethylcarbazole) (Vector Laboratories, Inc., Burlingame, CA, USA) was used according to the manufacturer's instructions (Narvaez et al. 2005).

Results

Treatment of Caco-2 cells with caspase inhibitors during RV infection decreases apoptotic nuclei

We previously showed that Caco-2 cells infected with RV increase the release of EVs, which when concentrated at 100,000×*g* are heterogeneous, some of them having typical features of exosomes (Barreto et al. 2010). For example, electron microscope observations showed that the EVs have heterogeneous size and shape compatible (between 30 and 90 nm cup shaped) and incompatible (more irregular EV in shape and size) with exosomes (Barreto et al. 2010). Because the virus induces apoptosis (Chaibi et al. 2005), this heterogeneity could be caused by the conjoint liberation of exosomes and apoptotic bodies. To determine if this was the case, initially, we analyzed the effect of caspase inhibitors on RV infection and the heterogeneity of these EV. First, we evaluated the effect of caspase inhibitors on apoptosis induced by RV by treating Caco-2 cells with the inhibitors z-VAD-fmk, z-DEVD-fmk, and z-LEHD-fmk, individually or in a cocktail at a concentration of 10 μM for 1 h. Subsequently, the cells were infected with RRV (moi of five) or treated with the control preparation (mock) both previously activated with trypsin for 45 min. The presence of apoptotic nuclei induced during infection was evaluated after 18 h, the peak of apoptotic nuclei detection (data not shown). Although the caspase inhibitors added individually at 10 μM were capable of inhibiting the percentage of apoptotic nuclei induced by the virus, the inhibitory effect was higher when the cells were treated with the inhibitors in a cocktail (data not shown). We next tested concentrations of 5, 10, and 20 μM of the cocktail (Fig. 1a, b). In all the experiments, the inhibitors were present during the infection. The caspase inhibitor cocktail at 10 and 20 μM induced a significant decrease (p= 0.007 and 0.015 Wilcoxon tests, respectively) in the number of apoptotic nuclei compared with those observed for the other treatments (Fig. 1b).

Treatment of Caco-2 cells with caspase inhibitors during RV infection does not affect viral replication or intracellular location and expression of markers associated with EVs

To determine if the caspase inhibitor cocktail affected viral replication, we evaluated by fluorescence microscopy if in infected cells the cocktail interfered with the intracellular detection of VP6 (Fig. 2a), and if it affected the production of infectious viral particles (Fig. 2b). The use of the cocktail of inhibitors at different concentrations did not affect either the expression of VP6 or the production of viral particles (Fig. 2).

The cocktail could also be altering the ability of the cells to produce exosomes. To evaluate if the treatment with inhibitors produces a change in the intracellular compartments responsible for the production of exosomes, such as multivesicular bodies of endolysosomal origin, the intracellular distribution of the CD63 present in the multivesicular bodies as well as in the exosomes (Bobrie et al. 2012a; Ostrowski et al. 2010) was evaluated by immunofluorescence in RV-infected cells treated or not with the caspase inhibitor cocktail at 10 μM. CD63 was distributed in a granular pattern around the nucleus (Fig. 2c) in cells with or without the treatment. In addition, the cocktail's effect on the global expression of CD63 and Hsc70 (a stress protein that is associated with exosomes) in the cells was determined by WB (Fig. 2d). Similarly, the presence of CD63 and Hsc70 does not vary in the presence of the caspase inhibitor cocktail at 10 μM; therefore, these inhibitors do not have an appreciable effect on the expression of these proteins in the cells (Fig. 2d).

Finally, levels of intracellular AChE measured in three independent experiments (Fig. 2e) were not different between infected cells treated or not with the inhibitor cocktail. However, non-infected cells had higher levels of intracellular AChE (Fig. 2e). This intracellular decrease of AChE during infection could be explained by our previous observation that infected cells release higher numbers of EVs to the medium than do non-infected cells (Barreto et al. 2010). Together, these results suggest that the apoptosis inhibitors do not interfere with viral replication or the formation of exosomes. However, we cannot disregard the fact that caspase inhibitors affect the release of exosomes. Due to the low efficacy in the recovery of EVs from non-infected cells, it is not possible to evaluate if caspase inhibitors per se affect the exosomes release in the cells.

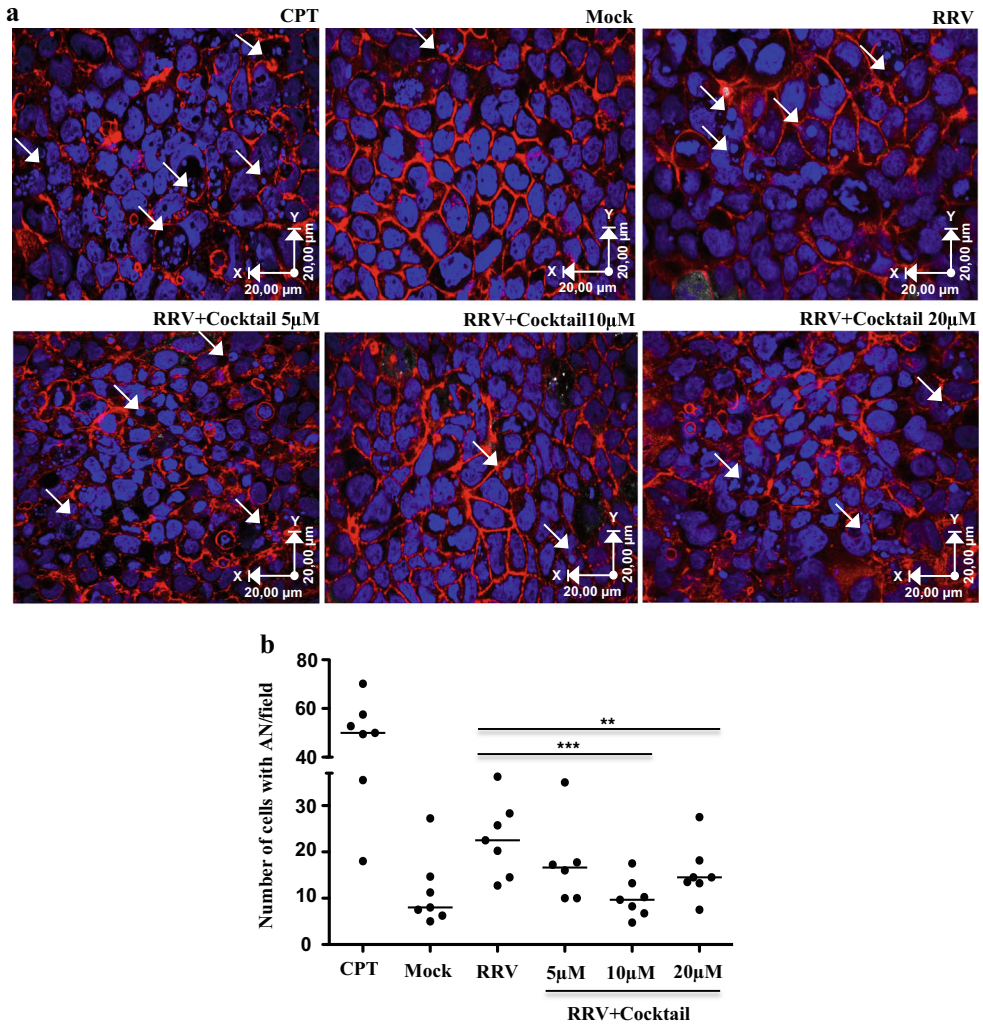

Fig. 1 Treatment of Caco-2 cells with caspase inhibitors during RV infection decreases apoptotic nuclei. Caco-2 cells cultured on microscope slides pretreated with collagen in DMEM supplemented with 20 % FBS for 10 days were treated with caspase inhibitors (z-VAD-fmk, z-DEVD-fmk, and z-LEHD-fmk) in a cocktail at different concentrations for 1 h and then infected for 45 min with the RRV strain (moi of five). The inhibitors were maintained during the virus inoculation and 18 h after infection. As a control of apoptosis induction, we use camptothecin (CPT). **a** Visualization of apoptotic nuclei (*white arrows*) in a representative image of seven independent experiments (nuclei dyed with DAPI (*blue*) and filamentous actin with phalloidin Alexa-fluor 594 (*red*)). The images were acquired with an Olympus FV-1000 confocal microscope. **b** Number of cells with apoptotic nuclei by field. The median of seven independent experiments is shown. Each single point represents the median of counting six different optical fields. The statistical significances are shown using non-parametric test for paired or non-paired data (Wilcoxon or Mann Whitney tests $p<0.05$*, $p<0.01$**, $p<0.001$***)

EV concentrated at 100,000×*g* produced by RV-infected Caco-2 cells decrease in the presence of caspase inhibitors

Using a filtration/ultracentrifugation protocol that concentrates EVs at 100.000×*g*, we previously showed that Caco-2 vesicles presented markers described for exosomes, such as CD63, Hsc70, MFG-E8, and AChE (Barreto et al. 2010; Bastos-Amador et al. 2012a; Bobrie et al. 2012a; Cantin et al. 2008; Johnstone et al. 1987; Mathivanan et al. 2010). To evaluate how apoptosis affects the production of EVs produced during RV infection, first, Caco-2 cells were cultivated for 15 days, and after 1 h of treatment with the caspase inhibitors cocktail, they were infected with RRV. At 24 h post-infection, the supernatants of the cells were collected to obtain the vesicles through a differential centrifugation protocol in which successive centrifugations at 4000×*g*, 10,000×*g*, and 100,000×*g* were performed to precipitate large vesicles from dead cells, microvesicles and exosomes, respectively (Thery et al. 2006). We used this protocol to expand the subsets of EV for analysis and evaluated Hsc70, CD63, and AChE in the EV obtained from infected cells cultured in the presence or absence of caspase inhibitors (Fig. 3 and data not shown).

Caspase inhibitors consistently decreased the vesicles that were concentrated at 100,000×*g* and expressed the markers Hsc70 and AChE, and they had variable effects on the EVs that were obtained at 4000×*g* and 10,000×*g* and expressed

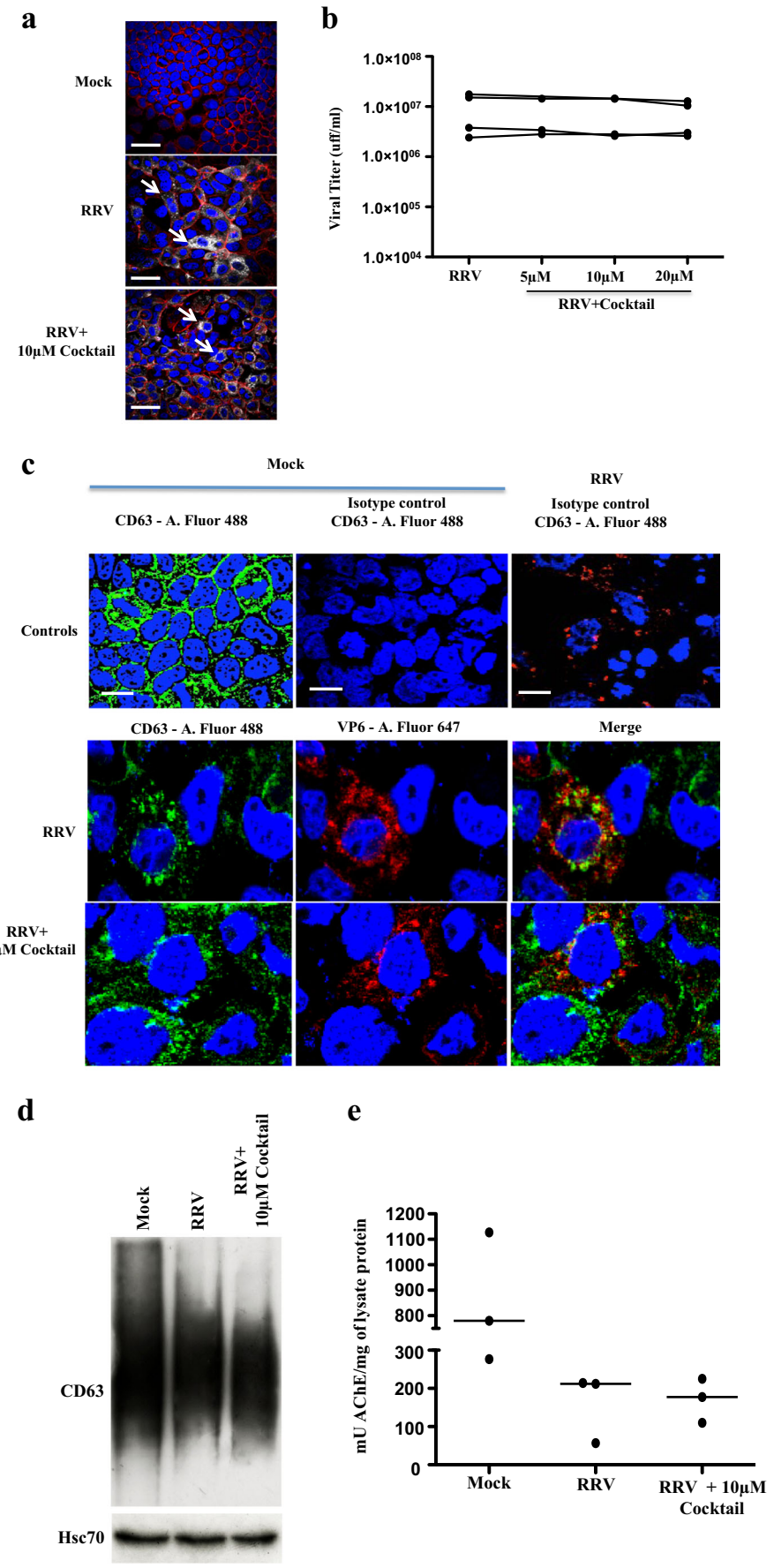

Fig. 2 The presence of caspase inhibitors during RV infection does not affect viral replication or the intracellular expression of CD63 and Hsc70 or AChE activity. Caco-2 cells cultivated as described were treated with the caspase inhibitor cocktail (10 μM de z-VAD-fmk, z-DEVD-fmk, and z-LEHD-fmk) for 1 h and then infected for 45 min with RRV (moi of five) or the control mock infection. The inhibitors were maintained during the virus inoculation and 18 h after the infection. **a** Cell nuclei were stained with DAPI (*blue*), filamentous actin were detected using phalloidin Alexa-fluor 594 (*red*), and VP6 was identified by using a Mab anti-VP6 followed by a mouse anti-IgG polyclonal antibody conjugated with Alexa-fluor 647 (*gray*). *White thick lines* correspond to 40 μm. *Arrows* show infected cells **b** The viral particles present in the supernatants of the treated cells were subjected to a viral titration assay by immunocytochemistry on MA104 cells. Each point represents the viral titter obtained for each condition. Results from 4 independent experiments are shown; points corresponding to the same experiment are connected by lines. **c** Cell nuclei were stained with DAPI (*blue*), and viral protein VP6 was identified using a Mab anti-VP6 followed by a mouse anti-IgG polyclonal antibody conjugated with Alexa-fluor 647 (*red*), and Mab anti-CD63 conjugated with FITC (*in green*). As an isotype control, an IgG1κ Mab was conjugated with FITC. A representative image of three independent experiments is shown. *White thick lines* correspond to 20 μm. **d** WB evaluation of CD63 and Hsc70 from cell lysates (20 μg of protein per row). A representative image of three independent experiments **e** AChE quantification showing the quantity of mU of AChE activity present in each mg of protein from samples of three independent experiments

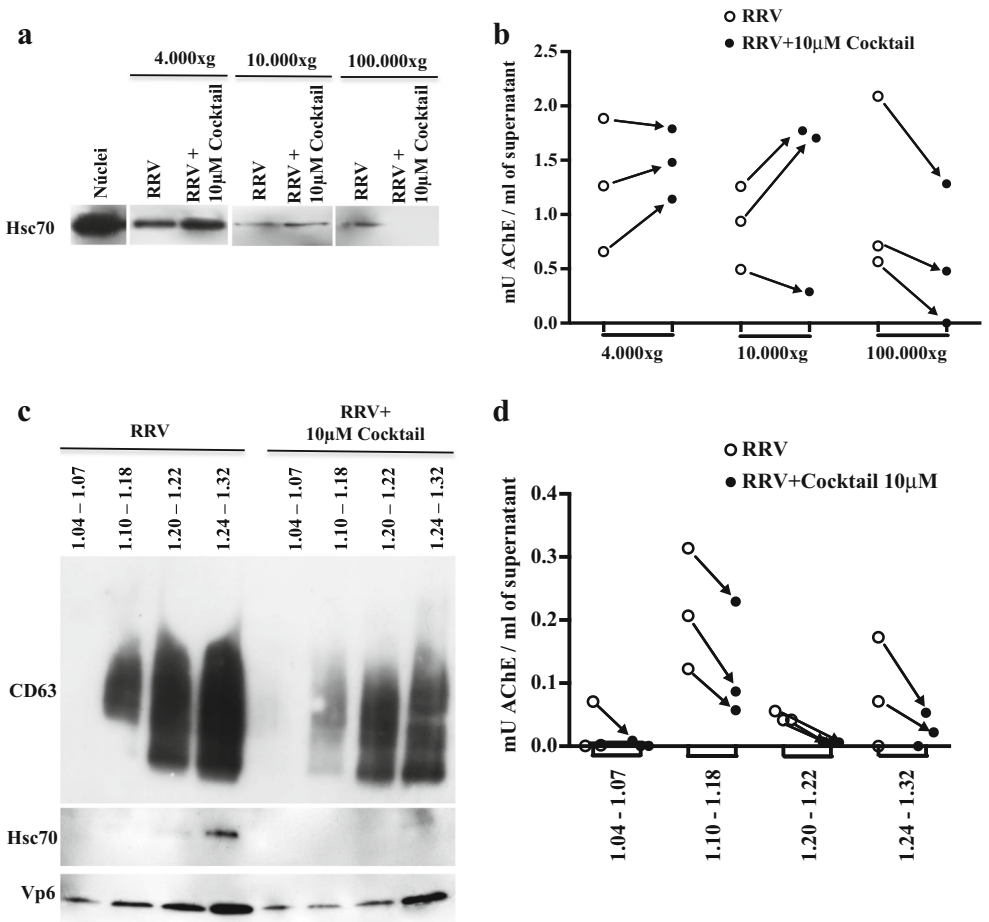

Fig. 3 In Caco-2 cells infected with RV and pretreated with caspase inhibitors apoptotic bodies sediment at 100,000×*g* and float along the sucrose gradient. Caco-2 cells cultured for 15 days were treated with a caspase inhibitor cocktail (10 μM of z-VAD-fmk, z-DEVD-fmk, and z-LEHD-fmk) for 1 h and then infected with RRV (moi of five) or treated with the infection control (mock) for 45 min. The inhibitors were maintained during the virus inoculation and for 24 h after the infection. Subsequently, the supernatants of the treated cells were subjected to a differential centrifugation protocol: 300×*g*, 4000×*g*, 10,000×*g*, and 100,000×*g* to eliminate cellular debris and large vesicles of dead cells, microvesicles and exosomes, respectively. The EVs were evaluated by WB to identify the presence of the marker Hsc70 (**a**) and were quantified through the measurement of AChE activity per ml of supernatant (**b**). A representative image of three independent WB experiments is shown. EVs obtained by the filtration protocol were separated in a linear sucrose gradient at 100,000×*g*. The obtained fractions were grouped in the following manner according to their buoyancy density (g/ml): FG1 1.04–1.06, FG2 1.10–1.18, FG3 1.20–1.22, FG4 1.24–1.32. *Left*, WB evaluation of CD63, Hsc70, and VP6 (**c**). A representative image of three independent experiments is shown. *Right*, AChE quantification (**d**). The quantity (mU) of AChE present per ml of supernatant is shown

these two markers (Fig. 3a, b). These results are consistent with those that we previously obtained with a filtration/ultracentrifugation protocol that concentrates the EV at 100.000×*g* (Barreto et al. 2010), and they suggest that apoptotic bodies are preferentially associated with the fraction obtained at 100,000×*g* (Fig. 3).

We next determined the buoyancy flotation of these EVs, because a density gradient exosomes have been shown to localize in fractions of densities between 1.10 and 1.18 g/ml, and apoptotic bodies in densities >1.24 g/ml (Thery et al. 2006, 2009). Taking into account that filtration/ultracentrifugation is more efficient than a differential centrifugation protocol (data not shown), we obtained EVs using this strategy, followed by a sucrose density gradient. After separating EVs in a linear sucrose gradient at 100,000×*g*, pools of 1-ml fractions were formed as follows: FG1 contained fractions with a low buoyant density between 1.04 and 1.08 g/ml; FG2 contained fractions with a density between 1.10 and 1.18 g/ml (where studies have typically located exosomes); FG3 contained fractions with an intermediate density between 1.20 and 1.22 g/ml; and FG4 contained fractions with a density >1.24 g/ml. In each pool of fractions, the presence of CD63, Hsc70, and VP6 was determined by WB, and the activity of AChE was evaluated (Fig. 3c, d). Contrary to our expectations, in 3/3 independent experiments, the caspase inhibitor cocktail at 10 μM caused all of the vesicle markers to decrease; this result was observed in the FG4 fractions, in which the apoptotic bodies had been previously reported, and also in the other fractions. These results suggest that apoptotic bodies have markers that also have been

described for exosomes and float in a sucrose density gradient between 1.10 and 1.32 g/ml; however, it is not possible to formally rule out that these caspase inhibitors also inhibit the formation of exosomes.

EV concentrated at 100,000×*g* produced by RV-infected Caco-2 cells contain histone H3 positive apoptotic bodies that have a high buoyant density on a sucrose gradient

In the few studies that have compared markers expressed by exosomes and apoptotic bodies, histones have been shown to be present only in the latter (Gutwein et al. 2005; Thery et al. 2001; Xie et al. 2009). Here, we compared the presence of Hsc70, CD63 (Fig. 4 a, b), and AChE (Fig. 4c) and the apoptotic body marker the histone H3 (Fig. 4d) on EV produced by infected and non infected cells obtained by the two purification methods previously described. Globally, and in agreement with previous results (Barreto et al. 2010), vesicles from RV-infected cells prepared by both filtration/ultracentrifugation and differential centrifugation presented higher amounts of CD63 protein (in 3/3 experiments, Fig. 4b) and AChE activity (Fig. 4c) compared with EV obtained from cells treated with the Mock control. CD63 (3/3 independent experiments) was preferentially found in the 100,000×*g* (Fig. 4b) vesicles, whereas Hsc70 and AChE (3/3 independent experiments) were found in all EV populations. Hsc70 (3/3 independent experiments) and AChE (5/8 independent experiments) proteins were found to significantly increase after infection in the EVs obtained at 4000×*g* (Fig. 4a, c, and data not shown). In the EVs obtained at 10,000×*g*, the increase of these proteins after infection was detected in 3/3 experiments for Hsc70 and only 4/8 independent experiments for AChE (Fig. 4a, c, and data not shown).

The H3 histone was detected by WB in both 100,000×*g* vesicles, prepared by filtration/ultracentrifugation and differential centrifugation, and at higher levels in EVs from infected cells compared with those from mock treated cells (Fig. 4d). Surprisingly, H3 was only slightly observed in EVs precipitated at 4000×*g* and not detected at 10,000×*g* (3/3 experiments) (Fig. 4d). Altogether, these experiments suggest that the EVs concentrated at 100,000×*g* are the most affected by RV infection and contain both exosomes and apoptotic bodies. Of note, in EVs from cells treated with caspase inhibitors described above, it was not possible to detect H3 (data not shown), most probably due to the sensitivity of the WB.

To determine the buoyant density of the apoptotic bodies identified by the presence of the H3 histone obtained from infected and non-infected cells, EVs were subjected to a filtration/ultracentrifugation protocol and separated in a linear sucrose gradient. From the gradient, pools of 1-ml fractions were obtained, as described above, and the presence of H3 was determined by WB (Fig. 4e). To increase sensitivity for the detection of the histone, these EVs were concentrated three times. H3 was preferentially observed in the high buoyant density fractions of EVs of infected cells in three independent experiments, and was not detected in the EV of the non-infected cells (Fig. 4e). Although there was a degree of variability between the experiments, Hsc70 had a tendency to present along all of the gradients in the EVs of the infected cells (Fig. 4e). In non-infected cells, Hsc70 tends to peak in the EV fractions between 1.10 and 1.18 g/ml respect to other fractions. These results suggest that the apoptotic bodies that were detected according to the presence of histone H3 are preferentially located in the 1.20–1.32 fractions, and thus, could be partially separated from the EVs with exosome features according to differences in buoyant density.

Discussion

In this study, we performed an analysis of the EVs released during RV infection of Caco-2 cells. These EVs are most probably composed of multiple kinds of vesicles that are difficult to characterize with precision. Here, we studied the heterogeneity of EVs produced by RV-infected cells focusing on exosomes and apoptotic bodies. First, EVs were obtained from cells cultured in the presence or absence of caspase inhibitors. We observed that in cells infected in the presence of caspase inhibitors, Hsc70 and AChE diminished in EVs obtained at 100,000×*g* and in both vesicles obtained by sucrose gradient with low and high buoyant densities, indicating that apoptotic bodies were present in those fractions. In the absence of caspase inhibitors, RV infection increased expression of CD63, Hsc70, and AChE in all of the EVs analyzed; however, CD63 preferentially localized in the 100,000×*g* fraction. Second, we evaluated the presence of the apoptotic body marker H3 in EVs, and we observed that this protein only increased in EVs concentrated at 100,000×*g* and with high buoyant densities on a sucrose gradient. Therefore, we refer to apoptotic bodies as EV that are concentrated at 100,000×*g* and present denser buoyant densities higher than 1.24 g/ml in linear sucrose gradients. Thus, RV infection increases the release of EVs that, upon concentration at 100,000×*g*, are composed by exosomes mixed with apoptotic bodies, which can be partially separated using sucrose gradients. These EVs can have potentially different immunomodulatory functions that should be studied further.

Using the RV-infected Caco-2 cell model, we previously obtained an EV population enriched in exosomes by a protocol that uses filtration followed by an ultracentrifugation step (Barreto et al. 2010). These EVs were shown to inhibit the viability and proliferation of CD4 T lymphocytes (Barreto et al. 2010). As has been reported for exosomes (Mathivanan et al. 2010; Thery et al. 2009), these EVs expressed CD63, Hsc70, MFG-E8, and AChE. However, the morphological characterization by electron microscopy

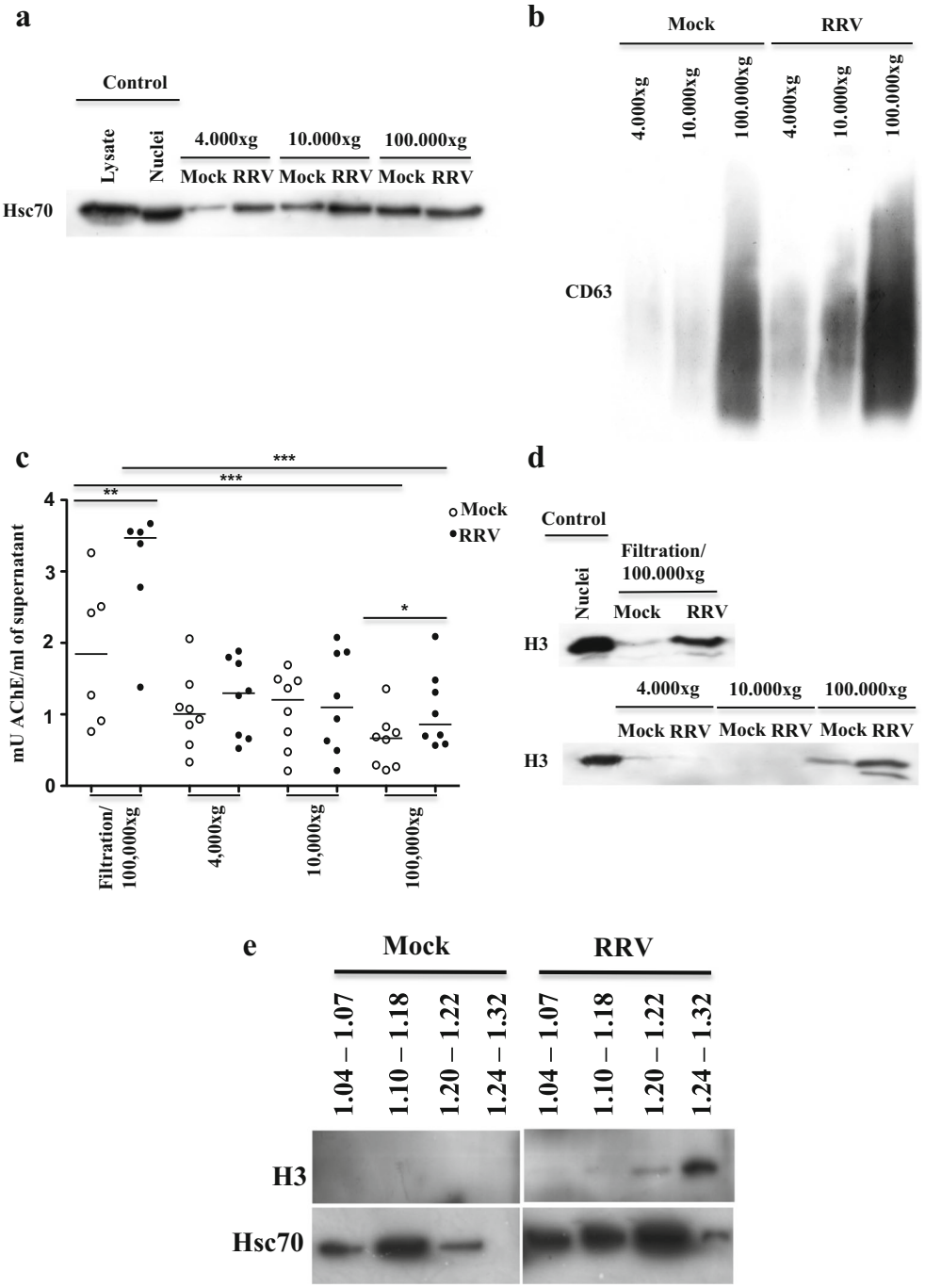

Fig. 4 Caco-2 cells infected with RV increase the release of histone H3-positive apoptotic bodies that concentrate at 100,000×*g* and have a high buoyant density on a sucrose gradient. Caco-2 cells cultured for 15 days in DMEM supplemented with 20 % FBS were infected with RRV (moi of 5) or treated with the control infection (mock) for 45 min. The supernatants were collected 24 h post-infection and were subjected to a differential centrifugation protocol (300×*g*, 4000×*g*, 10,000×*g*, and 100,000×*g*) to eliminate cellular debris and to obtain large vesicles derived from dead cells, microvesicles and exosomes, respectively, or filtration/ultracentrifugation to obtain exosomes. The EVs were evaluated by WB for the presence of **a** Hsc70 and **b** CD63; **c** AChE activity by fluorometry; **d** histone H3 by WB. Representative images of three independent experiments in the WB analysis are shown. For AChE activity, the median of five or six independent experiments analyzed by non-parametric statistical tests for paired and unpaired data (Wilcoxon or Mann Whitney tests $p<0.05$*, $p<0.01$**, $p<0.001$***) are shown. **e** Evaluation by WB of H3 and Hsc70 in EVs obtained by filtration/ultracentrifugation from non-infected Caco-2 cells (mock) and from infected cells (RRV) separated in a linear sucrose gradient in the absence of caspase inhibitors. A representative image of three independent experiments is shown

showed a heterogeneous population of EV: some of them having the typical cup-shape reported for exosomes (Van Niel et al. 2001) mixed with other irregular-shaped vesicles. In addition, in the sucrose gradients, we observed EV with densities typical of exosomes (between 1.10 and 1.18 g/ml) or described for apoptotic bodies (higher than 1.24 g/ml) (Barreto et al. 2010; Thery et al. 2001, 2009). However, considering that the virus induces an apoptosis process in vitro as well as in vivo (Bhowmick et al. 2012; Chaibi et al. 2005; Halasz et al. 2010; Martin-Latil et al. 2007), and the fact that the production of EV is performed in the absence of FBS (which could also increase the apoptosis in the system (Ricchi et al. 2003)), it is probable that apoptotic bodies occur in this model. Similarly, the sedimentation rates used to precipitate the exosomes may also precipitate apoptotic bodies; thus, it is probable that in the obtained EVs, these two types of vesicles occur.

Separating exosomes and apoptotic bodies in the supernatants of Caco-2 cells infected with RV is a difficult task, in part because an extensive characterization of apoptotic body

markers has not been performed. However, in some studies, apoptotic bodies have been found to have the same proteins as exosomes, with histones or the 14-3-3 protein as differential features (Gutwein et al. 2005; Thery et al. 2001; Xie et al. 2009). Because apoptotic bodies have been found to sediment in a wide range of *g* (between 1200 and 100,000×*g*) and have diverse sizes (Mathivanan et al. 2010; Thery et al. 2009), we initially decided to analyze the EVs produced during the RV infection using a differential centrifugation procedure to evaluate the presence of apoptotic bodies in the vesicles sedimenting at 4000×*g* (large vesicles of dead cells), 10,000×*g* (microvesicles), and 100,000×*g* (exosomes and most likely small apoptotic bodies) (Bobrie et al. 2012a; Crescitelli et al. 2013; Thery et al. 2006). Globally, we found Hsc70 and AChE in the three classes of EVs concentrated at 4000×*g*, 10,000×*g*, and 100,000×*g*, whereas CD63 protein preferentially occurred in the EVs concentrated at 100,000×*g* (Fig. 4b). Bobrie et al. (Bobrie et al. 2012a) found that while MFG-E8 protein was present in microvesicles and exosomes, CD63 was only found in exosomes. This fact highlights that CD63 is one of the best exosome markers. In our model, the presence of caspase inhibitors decreased the amount of CD63, associating this marker with apoptotic bodies (Fig. 3c). Recently, CD63 has been described in association with large apoptotic bodies as well as microvesicles and exosomes by flow cytometry (Crescitelli et al. 2013). However, we cannot formally rule out that the caspase inhibitors decrease exosome secretion.

Histone H3 expression was found to be increased in the vesicles from the cells infected with RV that were concentrated at 100,000×*g* (Fig. 4d); however, H3 was not clearly present in the larger EVs concentrated at 4000×*g*. Similar results were found for the EVs concentrated at 100,000×*g* by the filtration/ultracentrifugation protocol as well as by the differential centrifugation protocol, demonstrating that the presence of apoptotic bodies in the fraction containing the exosomes is not dependent on the protocol used for their purification. Unlike the H3 present in the nuclei, H3 that is found in EVs concentrated at 100,000×*g* presents an additional band of greater electrophoretic motility (Fig. 4d) that can reflect the presence of posttranslational modifications induced during apoptosis, because the isoforms of histones, such as H3 and H4, that have a higher degree of acetylation present a slightly faster motility on sodium dodecyl sulfate polyacrylamide gel electrophoresis (SDS-PAGE) (Georgieva and Sendra 1999). These hyperacetylated forms of histones may be induced during cell death by apoptosis (Dieker et al. 2007). Additionally, the methylation/demethylation processes of histone H3 can have a triggering role in the apoptosis process, according to the cell type and the methylated region (Cheng et al. 2009; Walter et al. 2014).

To reveal the effect of apoptosis in the EVs produced during RV infection, we obtained vesicles from the supernatants of infected cells in the presence of caspase inhibitors that have been shown to inhibit the generation of apoptotic bodies (Lemaire et al. 1998). Moreover, the cocktail of caspase inhibitors we used (z-VAD-fmk, z-DEVD-fmk, and z-LEHD-fmk) has been shown to inhibit apoptosis induced by RV (Martin-Latil et al. 2007). In the presence of this cocktail, Hsc70, CD63, and AChE were decreased in the fraction concentrated at 100,000×*g* (Fig. 3). These results, in addition to the location of histone H3, show that the apoptotic bodies that are generated in a caspase-dependent form are concomitantly concentrated with the exosomes at 100,000×*g*. Because apoptotic bodies have higher buoyant densities than exosomes (Thery et al. 2001), we decided to separate the EVs using a linear sucrose gradient. The observed decrease of CD63 and AChE in the presence of caspase inhibitors (Fig. 3c, d) may indicate that the apoptotic bodies have a similar buoyancy to that of exosomes or that inhibitors can decrease the production of exosomes. However, further studies are necessary to elucidate this. Interestingly, in the EVs of non-infected cells, a higher presence of Hsc70 was observed in the fractions of densities between 1.10 and 1.18 g/ml, characteristic of exosomes. In contrast, in the EVs of the infected cells, where a higher number of apoptotic bodies was expected, a robust Hsc70 expression was observed along the entire gradient (Fig. 4e). The histone H3 was consistently found only in the EVs of the infected cells and in the high-density fractions. In EVs concentrated at 100,000×*g*, other markers of apoptotic bodies, like 14-3-3 protein and histones H1, H2A, H2B, and H4, have also been found (Bautista 2015; Thery et al. 2001; Xie et al. 2009). Although caspase inhibitors decrease all the markers along the different fractions of the sucrose gradient (Fig. 3c, d), H3 localizes preferentially in the high-density fractions (Fig. 4e), indicating that this fraction is highly enriched in apoptotic bodies.

The high-density fraction (higher than 1.24 g/ml) of EV released by RV-infected cells (that we have shown here to contain H3 positive apoptotic bodies) inhibit proliferation and viability of T cells to a greater extent than the same EV from non-infected cells and inhibit the proliferation of T cells to a greater extent than EV with densities typical of exosomes from infected cells (Barreto et al. 2010). Thus, we speculate that RV infection may increase the release of early H3 positive apoptotic bodies with potentially unique immunomodulatory properties. It is possible that the EVs concentrated at 100,000×*g* and expressing histone H3 corresponded to early apoptotic bodies (Lane et al. 2005). At the beginning of apoptosis, plasma membrane blebbing generates small vesicles (small apoptotic bodies or microparticles) (Poon et al. 2014; Wickman et al. 2013) that contain histones (H3 included), which could have immunomodulatory properties. For example, extracellular histones H3 and H4 have an impact on the inflammatory response by directly inhibiting phagocytosis of the apoptotic cells and promoting the release of inflammatory

stimuli associated with secondary necrosis (Friggeri et al. 2012). In addition, acetylated histones have been reported to mediate macrophage activation (Pieterse et al. 2014).

Late apoptosis is accompanied by the exposition on the cell's surface of the material derived from the internal membrane systems, such as the endoplasmic reticulum (Franz et al. 2007). In EVs released by Caco-2 cells infected with RV concentrated at 100,000×*g*, the endoplasmic reticulum marker calnexin has not been detected (Barreto et al. 2010), also favoring the hypothesis that apoptotic bodies released 24 h after RV infection are from early stages. Histone H3 was not clearly detected in the vesicles concentrated at 4000×*g* where we expected to precipitate large apoptotic bodies; in addition, these vesicles did not present a decrease in the evaluated proteins when the cells were cultured in the presence of caspase inhibitors (Fig. 3a, b). In that sense, in our model, EVs concentrated at 4000×*g* can correspond to large apoptotic bodies derived from secondary necrosis.

Previously, we demonstrated that during RV infection of Caco-2 cells, there is an increased release of a heterogeneous population of EVs with the ability to inhibit the viability and proliferation of polyclonally stimulated CD4 T cells, depending, in part, on the TGF-β present in the EVs (Barreto et al. 2010; Rodriguez et al. 2012). Here, we have shown that in these EVs, there are, in addition to exosomes, apoptotic bodies expressing the histone H3 that have the potential to modulate the immune response. Further studies are necessary to better characterize these EV subsets and improve our understanding of their immunodulatory functions.

Acknowledgements This study was financed by the Pontificia Universidad Javeriana through the projects "Study of the mechanism in which microvesicles are released by intestinal cells infected by rotavirus inhibiting the function of the T lymphocyte" (ID 3693) and "Approach to the proteomic analysis of vesicular structures produced during the infection by rotavirus of intestinal epithelial cells" (ID 3104) and ID6331.

Conflict of interest No potential conflicts of interest of the authors were disclosed.

References

Barreto A, Gonzalez JM, Kabingu E, Asea A, Fiorentino S (2003) Stress-induced release of HSC70 from human tumors. Cell Immunol 222: 97–104

Barreto A, Rodriguez LS, Rojas OL, Wolf M, Greenberg HB, Franco MA, Angel J (2010) Membrane vesicles released by intestinal epithelial cells infected with rotavirus inhibit T-cell function. Viral Immunol 23:595–608

Bastos-Amador P et al (2012a) Capture of cell-derived microvesicles (exosomes and apoptotic bodies) by human plasmacytoid dendritic cells. J Leukoc Biol 91:751–758. doi:10.1189/jlb.0111054

Bastos-Amador P, Royo F, Gonzalez E, Conde-Vancells J, Palomo-Diez L, Borras FE, Falcon-Perez JM (2012b) Proteomic analysis of microvesicles from plasma of healthy donors reveals high individual variability. J Proteome 75:3574–3584. doi:10.1016/j.jprot.2012.03.054

Bautista (2015) Unpublished results

Bhowmick R et al (2012) Rotaviral enterotoxin nonstructural protein 4 targets mitochondria for activation of apoptosis during infection. J Biol Chem 287:35004–35020

Bobrie A, Colombo M, Raposo G, Thery C (2011) Exosome secretion: molecular mechanisms and roles in immune responses. Traffic 12: 1659–1668

Bobrie A, Colombo M, Krumeich S, Raposo G, Théry C (2012a) Diverse subpopulations of vesicles secreted by different intracellular mechanisms are present in exosome preparations obtained by differential ultracentrifugation. J Extracellular Vesicles 1:18397

Bobrie A et al (2012b) Rab27a supports exosome-dependent and -independent mechanisms that modify the tumor microenvironment and can promote tumor progression. Cancer Res 72:4920–4930

Boshuizen JA et al (2003) Changes in small intestinal homeostasis, morphology, and gene expression during rotavirus infection of infant mice. J Virol 77:13005–13016

Cantin R, Diou J, Belanger D, Tremblay AM, Gilbert C (2008) Discrimination between exosomes and HIV-1: purification of both vesicles from cell-free supernatants. J Immunol Methods 338:21–30

Chaibi C, Cotte-Laffitte J, Sandre C, Esclatine A, Servin AL, Quero AM, Geniteau-Legendre M (2005) Rotavirus induces apoptosis in fully differentiated human intestinal Caco-2 cells. Virology 332:480–490

Cheng MF, Lee CH, Hsia KT, Huang GS, Lee HS (2009) Methylation of histone H3 lysine 27 associated with apoptosis in osteosarcoma cells induced by staurosporine. Histol Histopathol 24:1105–1111

Choi DS et al (2007) Proteomic analysis of microvesicles derived from human colorectal cancer cells. J Proteome Res 6:4646–4655

Cocucci E, Racchetti G, Meldolesi J (2009) Shedding microvesicles: artifacts no more. Trends Cell Biol 19:43–51

Crescitelli R et al (2013) Distinct RNA profiles in subpopulations of extracellular vesicles: apoptotic bodies, microvesicles and exosomes. J Extracell Vesicles 2:20677

Dieker JW et al (2007) Apoptosis-induced acetylation of histones is pathogenic in systemic lupus erythematosus. Arthritis Rheum 56:1921–1933

Franz S et al (2007) After shrinkage apoptotic cells expose internal membrane-derived epitopes on their plasma membranes. Cell Death Differ 14:733–742

Friggeri A et al (2012) Extracellular histones inhibit efferocytosis. Mol Med 18:825–833

Georgieva EI, Sendra R (1999) Mobility of acetylated histones in sodium dodecyl sulfate-polyacrylamide gel electrophoresis. Anal Biochem 269:399–402

Gutwein P et al (2005) Cleavage of L1 in exosomes and apoptotic membrane vesicles released from ovarian carcinoma cells. Clin Cancer Res 11:2492–2501

Gyorgy B et al (2011) Membrane vesicles, current state-of-the-art: emerging role of extracellular vesicles. Cell Mol Life Sci 68:2667–2688

Halasz P, Holloway G, Coulson BS (2010) Death mechanisms in epithelial cells following rotavirus infection, exposure to inactivated rotavirus or genome transfection. J Gen Virol 91:2007–2018

Johnstone RM, Adam M, Hammond JR, Orr L, Turbide C (1987) Vesicle formation during reticulocyte maturation. J Biol Chem 262:9412–9420

Kalra H et al (2012) Vesiclepedia: a compendium for extracellular vesicles with continuous community annotation. PLoS Biol 10: e1001450

Lane JD, Allan VJ, Woodman PG (2005) Active relocation of chromatin and endoplasmic reticulum into blebs in late apoptotic cells. J Cell Sci 118:4059–4071

Lemaire C, Andreau K, Souvannavong V, Adam A (1998) Inhibition of caspase activity induces a switch from apoptosis to necrosis. FEBS Lett 425:266–270

Martin-Latil S, Mousson L, Autret A, Colbere-Garapin F, Blondel B (2007) Bax is activated during rotavirus-induced apoptosis through the mitochondrial pathway. J Virol 81:4457–4464

Mathivanan S, Ji H, Simpson RJ (2010) Exosomes: extracellular organelles important in intercellular communication. J Proteome 73: 1907–1920

Meckes DG Jr, Raab-Traub N (2011) Microvesicles and viral infection. J Virol 85:12844–12854

Narvaez CF, Angel J, Franco MA (2005) Interaction of rotavirus with human myeloid dendritic cells. J Virol 79:14526–14535

Ostrowski M et al (2010) Rab27a and Rab27b control different steps of the exosome secretion pathway. Nat Cell Biol 12:19–30, **sup pp 11-13**

Pieterse E, Hofstra J, Berden J, Herrmann M, Dieker J, van der Vlag J (2014) Acetylated histones contribute to the immunostimulatory potential of neutrophil extracellular traps in systemic lupus erythematosus. Clin Exp Immunol 179:68–74

Poon IK, Lucas CD, Rossi AG, Ravichandran KS (2014) Apoptotic cell clearance: basic biology and therapeutic potential. Nat Rev Immunol 14:166–180

Ricchi P, Palma AD, Matola TD, Apicella A, Fortunato R, Zarrilli R, Acquaviva AM (2003) Aspirin protects Caco-2 cells from apoptosis after serum deprivation through the activation of a phosphatidylinositol 3-kinase/AKT/p21Cip/WAF1pathway. Mol Pharmacol 64:407–414

Rodríguez LS, Barreto A, Franco M, Angel J (2009) Immunomodulators released during rotavirus infection of polarized Caco-2 cells. Viral Immunol 22:163–172

Rodriguez LS, Narvaez CF, Rojas OL, Franco MA, Angel J (2012) Human myeloid dendritic cells treated with supernatants of rotavirus infected Caco-2 cells induce a poor Th1 response. Cell Immunol 272:154–161

Simpson RJ, Lim JW, Moritz RL, Mathivanan S (2009) Exosomes: proteomic insights and diagnostic potential. Expert Rev Proteomics 6: 267–283

Thery C (2011) Exosomes: secreted vesicles and intercellular communications F1000. Biol Rep 3:15

Thery C, Boussac M, Veron P, Ricciardi-Castagnoli P, Raposo G, Garin J, Amigorena S (2001) Proteomic analysis of dendritic cell-derived exosomes: a secreted subcellular compartment distinct from apoptotic vesicles. J Immunol 166:7309–7318

Thery C, Duban L, Segura E, Veron P, Lantz O, Amigorena S (2002) Indirect activation of naive CD4+ T cells by dendritic cell-derived exosomes. Nat Immunol 3:1156–1162

Thery C, Amigorena S, Raposo G, Clayton A (2006) Isolation and characterization of exosomes from cell culture supernatants and biological fluids Curr Protoc Cell Biol Chapter 3:Unit 3 22

Thery C, Ostrowski M, Segura E (2009) Membrane vesicles as conveyors of immune responses. Nat Rev Immunol 9:581–593

Van Niel G, Raposo G, Candalh C, Boussac M, Hershberg R, Cerf-Bensussan N, Heyman M (2001) Intestinal epithelial cells secrete exosome-like vesicles. Gastroenterology 121:337–349

Walter D, Matter A, Fahrenkrog B (2014) Loss of histone H3 methylation at lysine 4 triggers apoptosis in Saccharomyces cerevisiae. PLoS Genet 10:e1004095

Wickman GR et al (2013) Blebs produced by actin-myosin contraction during apoptosis release damage-associated molecular pattern proteins before secondary necrosis occurs. Cell Death Differ. doi:10.1038/cdd.2013.69

Xie Y et al (2009) Tumor apoptotic bodies inhibit CTL responses and antitumor immunity via membrane-bound transforming growth factor-beta1 inducing CD8+ T cell anergy and CD4+ Tr1 cell responses. Cancer Res 69:7756–7766